Characterization of Forward Scattering Parameters from an Arbitrarily Shaped Cylinder by Near-Field Probing

Reuven Shavit, *Senior Member, IEEE*, Albert Cohen, and Eugene C. Ngai

***Abstract*—The forward scattering from an arbitrarily shaped cylinder is characterized by its scattering pattern and the induced field ratio (IFR). Accurate calculation of these parameters for arbitrarily shaped and composite beams is in many cases time consuming, therefore analytical approximations are used. A combined experimental and numerical procedure for evaluation of these parameters based on near-field probing is presented as an alternative. This procedure is shown to be far more accurate than the analytical approximations presently used in calculations of the total scattering effect of tuned sandwich radomes. The results obtained by this method verify well with the scattering characteristics computed analytically or numerically by method of moments.**

I. Introduction

LARGE sandwich radomes are assembled from many panels connected together forming seams. Those seams introduce scattering effects that degrade the overall electromagnetic performance of the antenna enclosed in the radome in terms of the transmission loss and radiation pattern. The complete analysis of the scattering effect from all the seams in front of the antenna's aperture is dependent on the scattering characteristics of the individual seam and the array contribution from all the seams. The scattering characteristics of the individual seam is determined by its forward scattering value and its scattering pattern. Kennedy [1] introduced the induced field ratio (IFR) parameter to describe the forward scattering effect from an arbitrarily shaped conductive or dielectric beam/seam. The IFR is defined as the ratio of the forward scattered field to the hypothetical field radiated in the forward direction by the plane wave in the reference aperture of width equal to the shadow of the geometrical cross section of the beam/seam on the incident wavefront [2]. Low IFR is an indication of low scattering effect in the forward direction. Kay [3] described the algorithm for the computation of the array factor of the scattering from metal beams in a metal space frame radome and a similar derivation was developed for the case of a sandwich radome made from panels with interconnecting seams [4]. The objective in the design of high performance radomes with seams is to reduce the IFR value of the individual seams and distribute the overall scattered energy from all the seams omnidirectionally by randomizing the seam array geometry on the radome.

Manuscript received March 10, 1994; revised December 13, 1994.

R. Shavit is with the Department of Electrical and Computer Engineering, Ben-Gurion University of the Negev, Beer Sheva 84105, Israel.

A. Cohen and E. C. Ngai are with the Electronic Space Systems Corp., Concord, MA 01742-4697 USA.

IEEE Log Number 9411449.

Rusch [2] developed the IFR concept and suggested an experimental procedure to measure its value in the far-field for an arbitrarily shaped cylinder. This procedure lacks the capability to measure the seam/beam scattering pattern. For canonical beam cross sections (circular and ellipse) analytical computations can be performed, but for arbitrarily shaped beams or tuned dielectric seams [5] this is a quite laborious and time consuming task, which often requires intense numerical computations like method of moments or finite elements. Consequently, in many practical instances to speed up the computation time an approximate method is adopted [4]. It consists of evaluation of the measured IFR (Rusch's method) and an approximate scattering pattern. The latter is equal to that of the radiation pattern from an equivalent aperture with the seam's shadow width. Our experience indicates that in the case of an untuned dielectric seam this is a valid approximation, while inaccurate for the scattering pattern of a tuned seam [5].

This paper presents a combined experimental and numerical procedure based on near-field probing to determine the scattering characteristics of a composite seam. The accuracy of the IFR value is comparable to that measured in the far-field by Rusch's method, but in addition it provides the scattering pattern. A similar measurement technique based on the standard near field probing technique, but for a stationary cylinder and a moving probe in front of a large phased array was suggested by Grimm and Hoffman [6]. The information on the seams scattering pattern is essential to refine the calculations of the total scattering effect from all the seams in a large sandwich radome. The IFR and the scattering pattern of the seam are computed from the collected data using a simple mathematical algorithm based on the fast Fourier transform (FFT).

II. Method Description

The schematic configuration of the test set-up is shown in Fig. 1. The transmitting antenna is a horn with aperture dimensions $A*B$ and linear polarization (parallel or perpendicular to the cylinder axis). The illuminated arbitrarily shaped cylinder is located in the far-field of the transmitting antenna. An open waveguide with aperture dimensions $a*b$ probes the near-field in the vicinity of the cylinder along x axis at a distance z_0. The distance z_0 is large enough ($>3\lambda$) to avoid multiple reflections between the probe and the cylinder. By the standard near-field procedure [6], [7] the probe moves in front of the cylinder and samples its near-field. In our suggested test set-up, the probe is stationary, and the cylinder, mounted on a positioner track,

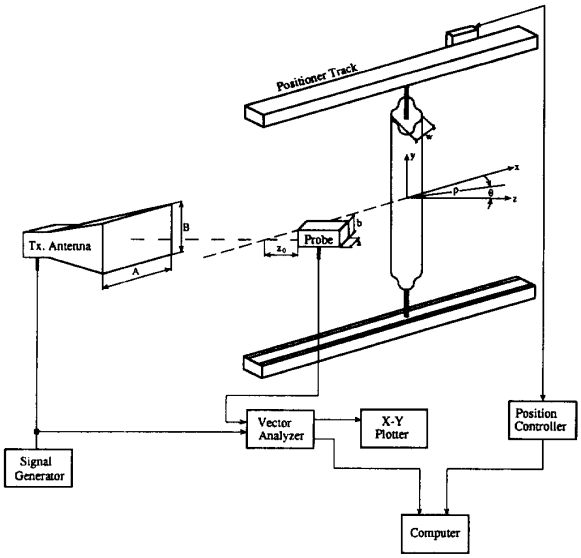

Fig 1. Schematic configuration of the measurement set-up.

moves in front of the probe. The position of the cylinder along the x axis and the amplitude and phase of the received signal are recorded. The system is calibrated before the cylinder movement, and the recorded signal $R_{y,x}(x, z_0)$ is referenced to this value. The subscripts y and x stand for vertical and horizontal polarizations of the incident field, respectively. The advantage of the suggested procedure is that it keeps the RF cables stationary and does not introduce measurement errors (amplitude and phase) throughout their motion as encountered in the standard near-field procedure. In the suggested procedure the incident angle of the illuminating field on the cylinder varies throughout the cylinder displacement. However, for relatively narrow cylinders and close proximity of the probe to the cylinder surface, the error is minimal and affordable.

A. Scattered Fields

Without loss of generality, we can assume that the incident field is y directed. Moreover, we assume that the cylinder is infinite in y direction, therefore all fields are only x and z dependent. The measured scattered field $E_y^s(x, z)$ by the cylinder can be expressed in terms of its plane-wave spectrum $\tilde{E}_y^s(k_x)$ and the plane-wave spectrum of the probe $\tilde{P}_y(k_x)$ [7]

$$E_y^s(x, z) = \int_{-\infty}^{\infty} \tilde{P}_y(k_x)\tilde{E}_y^s(k_x)e^{-jk_x x}e^{-jk_z z}\,dk_x \qquad (1)$$

where $k_z = \sqrt{k^2 - k_x^2}$ and k is the propagation constant in free space. In the current work, we have considered the probe correction to improve the accuracy of the computation of the scattered field from the near-field data as described by Yaghjian [7]. The Fourier inversion of (1) gives the scattered plane-wave spectrum of the cylinder in terms of the measured scattered near-field $E_y^s(x, z_0)$

$$\tilde{E}_y^s(k_x) = \frac{e^{jk_z z_0}}{2\pi}\,\tilde{P}_y^{-1}(k_x)\int_{s_a} E_y^s(x, z_0)e^{jk_x x}\,dx \qquad (2)$$

where s_a is the aperture domain along x axis on which the near-field is probed. Given the plane-wave spectrum $\tilde{E}_y^s(k_x)$, we can compute the scattered far-field $E_\phi^s(\rho, \theta)$ for $\rho \to \infty$ using the steepest descent path method [8]. In the far-field limit $k_x = k \sin\theta$ and $k_z = k\cos\theta$ in which θ is shown in Fig. 1. The result of such a derivation is

$$E_\phi^s(\rho, \theta) = 2\pi\sqrt{\frac{jk}{2\pi\rho}}\,e^{-jk\rho}\cos(\theta)\tilde{E}_y^s(k\cos\theta). \qquad (3)$$

Moreover, the plane-wave spectrum of the open waveguide probe is given by [8]

$$\tilde{P}_y(\theta) = \cos(\theta)\,\frac{\pi^2\cos\left(\frac{\pi a}{\lambda}\sin\theta\right)}{\pi^2 - 4\left(\frac{\pi a}{\lambda}\sin\theta\right)^2}. \qquad (4)$$

Substitution of (2) and (4) into (3) yields the scattered far-field pattern $F_y^s(\theta)$ of the cylinder in terms of the near-field data for vertical polarization

$$F_y^s(\theta) = \frac{\pi^2 - 4\left(\frac{\pi a}{\lambda}\sin\theta\right)^2}{\pi^2\cos\left(\frac{\pi a}{\lambda}\sin\theta\right)} \cdot \int_{s_a} E_y^s(x, z_0)e^{jkx\sin\theta}\,dx. \qquad (5)$$

By a similar derivation, with the appropriate plane-wave spectrum of the open waveguide probe [9] for perpendicular polarization to the cylinder axis, we obtain the cylinder scattering pattern $F_x^s(\theta)$ for horizontal polarization

$$F_x^s(\theta) = \frac{1 + \frac{\beta}{k}}{1 + \frac{\beta}{k}\cos\theta}\,\frac{\frac{\pi b}{\lambda}\sin\theta}{\sin\left(\frac{\pi b}{\lambda}\sin\theta\right)} \cdot \int_{s_a} E_x^s(x, z_0)e^{jkx\sin\theta}\,dx \qquad (6)$$

in which β is the propagation constant in the open waveguide for the dominant TE_{10} mode.

B. IFR Computation

The $IFR_{y,x}$ is defined as the ratio of the forward scattered far-field $E_{y,x}^s(\rho, 0)$ to the hypothetical far-field $E^r(\rho, 0)$ radiated in the forward direction by the plane wave E^{inc} in the reference aperture of width w equal to the shadow of the geometrical cross section of the cylinder on the incident wavefront [2]. The hypothetical field $E^r(\rho, \theta)$ can be obtained from (2) and (3) with E^{inc} as the aperture field. Following these steps we obtain

$$E^r(\rho, 0) = E^{inc}w\sqrt{\frac{jk}{2\pi\rho}}\,e^{jkz_0}e^{-jk\rho}. \qquad (7)$$

The ratio of (3) for $\theta = 0$ and (7) gives the $IFR_{y,x}$ of the cylinder in terms of the near-field data

$$IFR_{y,x} = \frac{1}{w}\int_{s_a}\frac{E_{y,x}^s(x, z_0)}{E^{inc}}\,dx. \qquad (8)$$

The near-field scattered by the cylinder $E^s_{y,x}(x, z_0)$ is related to the normalized recorded data, $R_{y,x}(x, z_0)$, through the relation $E^s_{y,x}(x, z_0)/E^{inc} = R_{y,x}(x, z_0) - 1$. Equations (5), (6), and (8) represent the basis for the suggested method and include the information on the IFR and the scattering pattern. Numerical examples are presented in the next section.

III. Numerical Results

A simple mathematical algorithm can be used to evaluate the integrals involved in the scattering pattern of the cylinder. Equations (5) and (6) are Fourier type and can be evaluated efficiently by the FFT algorithm. If we denote

$$I(\theta) = \int_{s_a} E^s(x, z_0) e^{jkx \sin\theta}\, dx \tag{9}$$

$I(\theta)$ can be rewritten as

$$I_m = \Delta x \sum_{i=0}^{N-1} E^s(x_i) e^{-jm\Delta k i \Delta x} \tag{10}$$

where

$$k_m = m\Delta k = k \sin(\theta_m): \qquad x_i = i\Delta x \tag{11}$$

and

$$\Delta k = \frac{2\pi}{N\Delta x}: \qquad N = 2^p: \quad p - \text{integer}$$
$$\Delta x - \text{spacing between near field sampling points.} \tag{12}$$

In the visible range of the scattering pattern $-k < k\sin(\theta_m) < k$.

During the course of this work we have compared the computed scattering pattern of the cylinder, based on the near-field data to the standard approximation often used in the scattering analysis of space frame radomes [4] and to the results predicted by the method of moments. The approximate forward scattering pattern, $F_a(\theta)$, is equal to the radiation pattern from an equivalent aperture with the cylinder shadow width w and with constant field distribution. Its analytical form is

$$F_a(\theta) = \frac{\sin\left(\pi \frac{w}{\lambda} \sin\theta\right)}{\pi \frac{w}{\lambda} \sin\theta} \tag{13}$$

where θ is measured relative to the angle of the incident wave.

To confirm the validity of the near-field approach, we have measured and computed the scattering pattern and IFR of a metal circular cylinder with 0.75" diameter, a dielectric rectangular beam with $\varepsilon_r = 4.2$ and dimensions 0.66"×2.25", and an untuned and tuned dielectric seam with dimensions 4.0" x 0.4" and $\varepsilon_r = 4.2$. The seam is tuned with a grid of conductive strips located on its center line, spaced 0.25" apart and with strip width of 0.062". The dielectric seam interconnects two type-A sandwich panels. Its cross-section is arbitrary and made of composite materials. The measurements were performed at 10 GHz for both vertical (VP) and horizontal (HP) polarizations.

Fig. 2 shows typical recorded near-field signals (amplitude and phase) for both vertical and horizontal polarizations in the course of the metal circular cylinder motion. Similar signals have been obtained in the other cases. The abscissa represents the relative distance along x axis from the line connecting the transmitting horn and the probe. One can notice the level of the reference signal, $R_{y,x}(x, z_0)$, before the cylinder crosses this line and the diffraction effect, when the cylinder begins to cross this line. The recorded signal is symmetric with respect to the boresight line. Based on the near-field data accumulated as shown above, one can compute the IFR and the scattering pattern. The result of such calculation is illustrated in Fig. 3. In the forward scattering direction (θ = 0) the amplitude of the scattered field is equal to $E^s(0) = 20 \log |\text{IFR} * w/\lambda|$. For comparison we present also the approximate scattering pattern and the exact analytical scattering pattern for the circular cylinder [10]. Both polarizations are shown. In the computation based on the near-field data we have used N = 256 sampling points and the spacing between sampling points was less than the Nyquist criterion $\lambda/2$. There is a reasonable agreement among the three traces. Fig. 4 makes the same comparison for the dielectric beam with the plane-wave illuminating the narrow width of the beam and its propagation direction normal to the beam axis. In this case the scattering pattern based on the near-field data is compared to the approximate pattern and to the scattering pattern computed by the method of moments [11]. The results again show a reasonable agreement among the patterns.

As an additional test case, we have considered the scattering characteristics of an untuned and tuned composite dielectric seam interconnecting two type-A sandwich panels. In this instance, the sandwich panels with the composite seam have been moved in front of the transmitting horn and the probe. The system is calibrated before the panel crosses the boresight line connecting the transmitting horn and the probe. We obtain the panel insertion phase delay and its transmission loss, when the panel crosses the boresight line and the seam scattering effect, when the seam crosses this line. Therefore, to obtain the net scattering effect of the seam relative to the panel, we subtract the insertion phase delay and the transmission loss of the panel from the measured near-field data. Fig. 5 shows the comparison of the scattering pattern (vertical polarization) for the untuned seam based on the near field data and the approximate form given by (13). One can observe that the scattering pattern has a definitive main beam and the first sidelobe is approximately 18 dB down. The main beam is in relatively reasonable agreement with the approximate form and less agreement is noticed in the sidelobes. This discrepancy may be attributed to multiple reflections between the probe and the seam. In this case the major effect on the antenna enclosed in the radome is due to the seam's scattering main beam, therefore use of the approximate form may result in good predictions of the radome performance [4]. Fig. 6 shows the same comparison for the tuned seam. The IFR in the tuned case (θ = 0 degrees) is lower than the value in the untuned case. Subsequently, the scattering level in an angular sector around the forward direction is reduced. The scattering pattern based on the near field data has no definitive main beam, while the approximate pattern predicts such a behavior. Here the approximate scattering pattern differs significantly from the computed pattern based on the near-field data. This

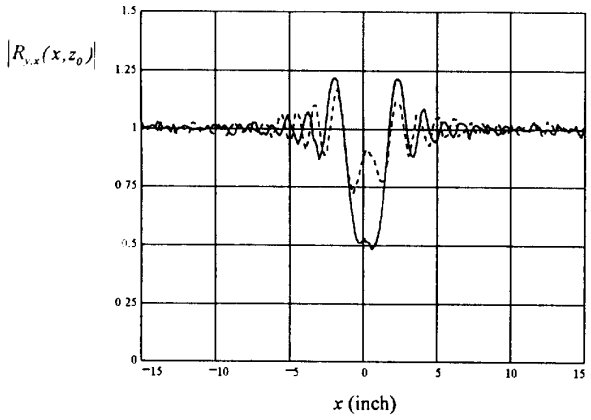

(a)

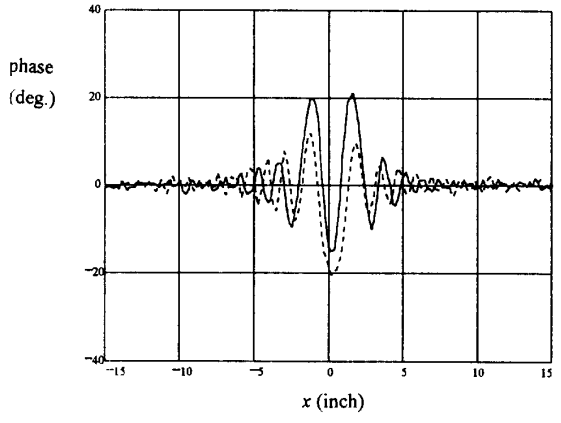

(b)

Fig. 2. Recorded signal throughout the metal cylinder motion.

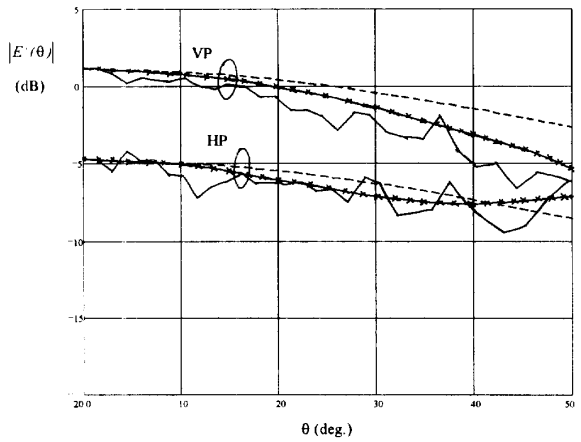

Fig. 3. Scattering pattern of a metal cylinder with diameter 0.75" (—) based on near field data, (-×-×-) exact solution [9], (- - - -) approximate form (13).

result may affect the prediction accuracy of the radome effect on the far-out sidelobes of the antenna.

Table I compares the IFR values at $\theta = 0$ degrees based on the accumulated near-field data to the IFR far-field values measured by Rusch's method [2] and to the computed values.

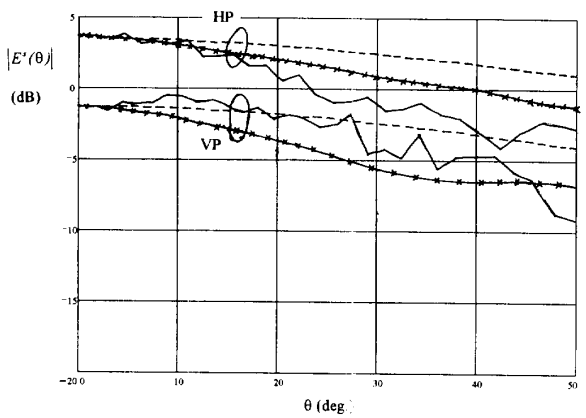

Fig. 4. Scattering pattern of a rectangular dielectric beam 0.66"×2.25" (—) based on near field data, (-×-×-) method of moments solution [10], (- - - -) approximate form (13).

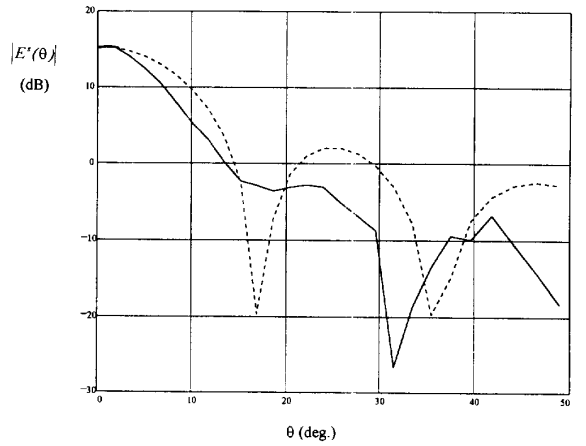

Fig. 5. Scattering pattern (vertical polarization) of an (—) untuned dielectric seam, (- - - -) approximate form (13).

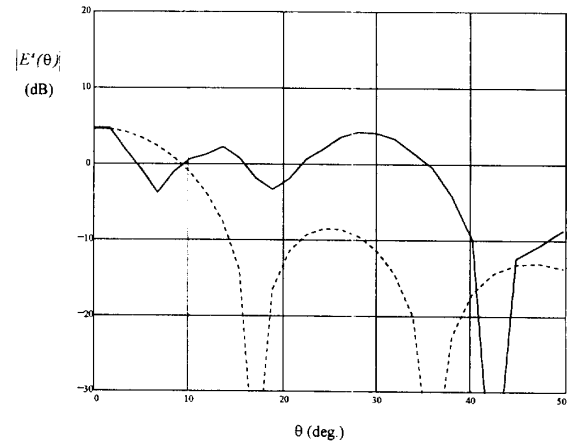

Fig. 6. Scattering pattern (vertical polarization) of a (—) tuned dielectric seam, (- - - -) approximate form (13).

These IFR's have been computed from the scattered fields as discussed by Kennedy [1]. The scattered fields for the

TABLE I
COMPARISON OF IFR VALUES FOR ALL THE TESTED BEAMS/SEAMS

	Vertical Polarization			Horizontal Polarization		
Beam Type	Computed	Measured Near-Field	Measured Far-Field	Computed	Measured Near-Field	Measured Far-Field
Metallic Circular Cyl. 0.75" diam	-1.31+j0.55	-1.37+j0.64	-1.25+j0.52	-0.68-j0.33	-0.72-j0.26	-0.69-j0.36
Plastic Beam 0.66" x 2.25"	-0.73-j0.34	-1.03-j0.81	-0.97-j0.18	-1.71+j0.93	-2.25+j0.41	-1.80+j0.49
Untuned Seam 4.0" x 0.4"	N/A	-1.06-j1.02	-1.12-j0.38	N/A	-0.8-j0.85	-1.15-j0.35
Tuned Seam 4.0" x 0.4"	N/A	-0.36-j0.23	-0.305-j0.1	N/A	-0.11-j0.07	-0.32-j0.02

metallic cylinder are computed analytically as discussed by Harrington [10], while the scattered fields of the rectangular plastic beam are computed numerically by the method of moments as discussed by Richmond [11].

We can observe a reasonable agreement among the measured IFR values by both methods and the computed values. In conclusion, the suggested method is similar in accuracy with the far-field method for the IFR measurement, but in addition, it provides important information on the beam/seam scattering pattern.

IV. SUMMARY

A new procedure, based on near-field probing, for the scattering analysis of arbitrarily shaped and composite cylinders have been presented. The method is general and determines the scattering pattern and the IFR. It complements Rusch's method, which determines only the IFR value, based on far-field measurement. The approach verifies well with the exact scattering characteristics computed analytically and by the method of moments. It delivers the scattering characteristics in a short period of time. For specific composite and arbitrarily shaped beams the suggested approach is the only option. The information obtained on the scattering pattern helps to refine the calculations of the scattering analysis of large space frame radomes.

ACKNOWLEDGMENT

The authors wish to express their thanks to C. Slotta from ESSCO, Concord, MA for performing the measurements during the course of this work.

REFERENCES

[1] P. D. Kennedy, "An analysis of the electrical characteristics of structurally supported radomes," Ohio State Univ. Rep. under Contract AF-30 (602)-1620, Nov. 1958.
[2] W. V. T. Rusch, J. A. Hansen, C. A. Klein, and R. Mittra, "Forward scattering from square cylinders in the resonance region with application to aperture blockage," *IEEE Trans. Antennas Propagat.*, vol. AP-24, no. 2, pp. 182–189, Mar. 1976.
[3] A. F. Kay, "Electrical design of metal space frame radomes," *IEEE Trans. Antennas Propagat.*, vol. AP-13, pp. 188–202, Mar. 1965.
[4] R. Shavit, A. P. Smolski, E. Michielssen, and R. Mittra, "Scattering analysis of high performance large sandwich radomes," *IEEE Trans. Antennas Propagat.*, vol. 40, no. 2, pp. 126–133, Feb. 1992.
[5] E. Michielssen and R. Mittra, "TE plane wave scattering by a dielectric cylinder loaded with perfectly conducting strips," in *Symp. Dig. IEEE Conf. Antennas Propagat.*, Dallas, TX, May 1990, pp. 125–128.
[6] K. R. Grimm and J. B. Hoffman, "Measurement of small radar target forward scattering by planar near field scanning," in *Symp. Dig. Conf. on Precision Electromagnetic Measurements*, Gaithersburg, MD, 1986, pp. 1–3.
[7] A. D. Yaghjian, "An overview of near-field antenna measurements," *IEEE Trans. Antennas Propagat.*, vol. AP-34, no. 1, pp. 30–45, Jan. 1986.
[8] L. B. Felsen and N. Marcuvitz, *Radiation and Scattering of Waves*. Englewood Cliffs, NJ: Prentice-Hall, 1973.
[9] A. D. Yaghjian, "Approximate formulas for the far field and gain of open-ended rectangular waveguide," *IEEE Trans. Antennas Propagat.*, vol. AP-32, no. 4, pp. 378–384, Apr. 1984.
[10] R. F. Harrington, *Time-Harmonic Electromagnetic Fields*. New York: McGraw-Hill, 1961.
[11] J. H. Richmond, "Scattering by a dielectric cylinder of arbitrarily cross-section shape," *IEEE Trans. Antennas Propagat.*, vol. AP-13, pp. 334–341, May 1965.

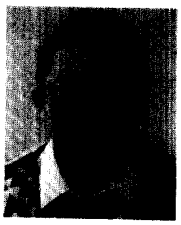

Reuven Shavit (M'82–SM'90) was born in Rumania on Nov. 14, 1949. He received the B.S. and M.S. degrees in electrical engineering from the Technion, Israel, in 1971 and 1977, respectively, and the Ph.D. degree in electrical engineering from the University of California, Los Angeles, in 1982.

From 1971 to 1993 he worked as a Staff Engineer and Antenna Group Leader in the Electronic Research Laboratories of the Israeli Ministry of Defense, Tel Aviv, where he was involved in the design of reflector, microstrip, and slot antenna arrays. He was also a part-time Lecturer at Tel Aviv University, teaching various antenna and electromagnetic courses. From 1988–1990 he was associated with ESSCO, Concord, MA, as a Principal Engineer involved in scattering analysis and tuning techniques of high performance ground based radomes. Currently, he is with Ben-Gurion University of the Negev, as a Lecturer doing research in microwave components and antennas. His current research interests are in the areas of tuning techniques for radomes and numerical methods for design microstrip, slot, and reflector antennas.

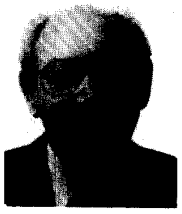

Albert Cohen was born in Boston, MA on October 14, 1927. He received the B.S. in electrical engineering in 1951 from the Massachusetts Institute of Technology. He received the Master of Science degree in engineering management from Northeastern University in 1964.

He worked with Gabriel Laboratories in 1951 and became Senior Research Engineer. In 1955, he joined the technical staff of MIT Lincoln Laboratory, and became Group Leader. In 1961, he co-founded Electronic Space Systems Corporation (ESSCO) of Concord, MA, a high technology company specializing in the research, development, design, and manufacture of aerospace ground equipment of which he became President and Chief Executive Officer in 1964. Presently he is Chairman of the Board and Chief Executive Officer of ESSCO. He also serves as Chairman of the Board of ESSCO Collins, Ltd. in Ireland, ESSCO's manufacturing subsidiary in the European Common Market and is a member of the Board of Directors of Unifirst Corporation. He has authored several articles for various technical journals. A representative paper, "A 150-Foot Metal Space Frame Radome" WADC Technical Report 57–314 ASTIA Document AD130929, vol. 1, June 1957, described the first utilization of metallic beams in a triangulated spherical large ground radome exhibiting extremely large bandwidth. This design concept was implemented as what is now known as the "Haystack Radome" and has been adopted worldwide in over a thousand applications.

Mr. Cohen has received a number of awards, is a Registered Professional Engineer in the Commonwealth of Massachusetts, and is a member of several professional and technical societies.

Eugene C. Ngai was born in Shanghai, China. He received the B.S.E.E. degree from Northwestern University, Evanston, IL in 1978, and the electrical engineer degree from Syracuse University, Syracuse, NY in 1980.

From 1980 to 1984, he was with RCA Astro-Electronics, Princeton, NJ, engaged in the design and analysis of antenna for geosynchronized satellite application and direct broadcasting activities and the study of reconfigurable antenna systems employing active feed elements in offset parabolic and dual-reflector antenna. From 1984 to 1988, he was with Raytheon Equipment Division Laboratories, working in the area of radar and microwave propagation, engaged in the development of adaptive array and high resolution imaging radar. In 1988, he joined Electronic Space Systems Corporation (ESSCO), where he is currently a Senior Principal Engineer engaged in the design and analyses of spaced frame radomes and wideband sandwich radomes for radar and communication application, working in the area of spherical near field measurement for far-field transformation and microwave holographic technique for precision reflector panel alignment. He has engaged extensively on the study of radome electromagnetic scattering effect by using advanced numerical techniques; e.g., the method of moment and the finite element method. He has worked on the design and development of Very Large Compact Range Reflector for RCS and antenna measurements. His research interests include FSS, adaptive array, electromagnetic interference, and numerical and measurement techniques.